PAPER • OPEN ACCESS

Design of a roll autopilot for a skid-to-turn guided missile

Recent citations

- Ahmed Fathi Sobh *et al*

View the article online for updates and enhancements.

Design of a roll autopilot for a skid-to-turn guided missile

K M Ali[1], M Abozied, I Arafa and Y Z Elhalwagy

Military Technical College, Cairo, Egypt

[1] E-mail: kimo.004990 @gmail.com

Abstract. the design of autonomous systems is a growing research field which attract an increasing interest in various civilian and military applications. The design of control system can be considered a leading factor for developing any autonomous system. In this paper devoted to a missile autopilot which should achieve specific characteristics and performance criteria to ensure the overall system stability to track the desired commands in the presence of high dynamics and different uncertainties with high accuracy. The investigation of accurate missile 6DOF model is developed and linearization has been performed for designing the proper controllers for the pitch and roll channels and choose the optimum trim points based on system dynamic pressure. A design of lead compensator classical controller is presented to meet certain requirement of both time and frequency characteristic to ensure the system stability. The designed autopilot is evaluated using Matlab simulation is carried out for evaluating the proposed missile autopilot controller performance, the proposed controller presented sufficient performance during flight and simplicity, reliability, and availability for implementation in real time applications.

Keywords: Autopilot design, classical control, system stability, Linearization, Modeling.

Nomenclature

a_n	Normal acceleration	N_ζ	Yawing moment due to rudder angle
a_{nc}	Commanded normal acceleration	P	Position vector
B	Transformation matrix from Earth axes top, q, r body axes	top, q, r	Roll, pitch and yaw rates
		Q	Dynamic pressure
C_D	Coefficient of drag	q_c	Commanded pitch rate
C_L	Coefficient of lift	S	Reference area
C_l	Coefficient of rolling moment	s	Laplace operator
C_m	Coefficient of pitching moment	T_s	Sampling time
C_n	Coefficient of yawing moment	t	Time
$Cx_By_Bz_B$	Body axes	t_r	Rise time
C_Y	Coefficient of side force	t_s	Settling time
D	Drag force, Missile diameter	u, v, w	Velocity component in body axes
e_q	Error in pitch rate	u	Input signal
F_B	Resultant of external forces w.r.t. body axes	u_0	Undisturbed longitudinal velocity
g	Gravitational acceleration	u_η	Control signal
H	Altitude	V	Total velocity
H_B	Angular momentum w.r.t. body axes	v_B	Velocity w.r.t. body frame
I_{xx}, I_{yy}, I_{zz}	Moments of inertia about body axes	X_u	Axial force due to longitudinal velocity
I_{xy}, I_{zy}, I_{xz}	Product of moments of inertia about bodyx, y, z axes		Position of body c.g. w.r.t. Earth axes

i_B, j_B, k_B	Body axes unit vectors	Y	Side force
J	Inertia tensor	Y_r	Side force due to yaw rate
K_a	Normal acceleration gain	Y_v	Side force due to side velocity
K_q	Pitch rate gain	Y_ζ	Side force due to rudder angle
k	Sample number	y	Output vector
L	Lift force, Rolling moment	Z_q	Normal force due to pitch rate
L_p	Rolling moment due to roll rate	Z_w	Normal force due to vertical velocity
L_ξ	Rolling moment due to aileron angle	Z_α	Normal force due to angle of attack
l_p	Position of accelerometer in front of c.g.	Z_η	Normal force due to elevator angle
M	Pitching moment, Resultant of external moments w.r.t. body axes	α	Angle of attack
M. O.	Maximum percentage overshoot	β	Side slip angle
Ma	Mach number	ζ	Rudder angle
M_q	Pitching moment due to pitch rate	ζ_{sp}	Short period mode damping ratio
M_w	Pitching moment due to vertical velocity	η	Elevator angle
M_α	Pitching moment due to angle of attack	θ	Pitch angle
M_η	Pitching moment due to elevator angle	ξ	Aileron angle
m	Missile mass	ρ	Air density
N	Yawing moment	φ	Roll angle
N_2	Prediction horizon	ψ	Yaw angle
N_r	Yawing moment due to yaw rate	ω_B	Angular velocity w.r.t. body frame
N_u	Control horizon	ω_n	Short period mode natural frequency

Introduction

The design of autopilots to ensure that the missile achieves accelerations as commanded and maintains stability with enough stability margins[1][2]. Before going into mathematical detail concerning the motion of the missile in space as a result of guidance commands, some definitions and discussion are desirable, including:

- The missile will maneuver by moving control surfaces, in our case the control surfaces are aerodynamic rudders (aerodynamic control) [1][2].
- The control method is called skid-to-turn (STT) control method. This means that if the guidance system "sees" the missile at point which is far to the right and low from its desired point, the guidance angular error detector produces two signals, a right-left signal and a down-up signal which are transmitted to two separate servos, rudder servos and elevator servos. Alternatively, it calculates the resultant of the two signals needed to be contributed for all the four servos.
- The missile will not roll freely and its orientation in roll must be controlled. As the higher roll rate affects the rate of other angular velocities so the controller should maintain the rolling angle to zero and damp any roll rate.
- The guidance of the missile c.g. in space will be performed using the control of lateral and normal acceleration utilizing the change in the
- angle of attack and sideslip angle under the effect of fins deflection.

The control system consists of a roll autopilot and two essentially identical pitch and yaw autopilots. The guidance system detects whether the missile c.g. is flying high or low, or much to the
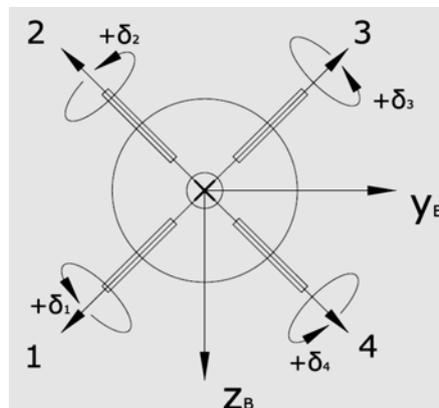
left or right. Then, it measures these missile-position deviations or errors and applies them to the control system to reduce these errors to zero[3,4,5]. The task of the autopilot is to stabilize and guide the missile via fin deflections, which cause the missile body to rotate and hence translate into a new position. The fin servos respond to the commands ordered by the autopilot, and the actual fin deflection is that one which corresponds and satisfies the required maneuver. In all cases the servo torque should always overcome the hinge moment. These fin deflections then act as a forcing function to the airframe dynamic model.

Therefore, the main task of the autopilot subsystem can be summarized as follows:

- Ensure the desired acceleration characteristics for tracking guidance commands with high performance with sufficient system stability.
- Disturbance rejection in roll and pitch channels for the working flight envelop.

The missile actuation can be achieved by accurately controlling the fins surfaces angles where the control commands require the convention of positive surface deflection angles as shown in Fig.1 because there are four fins ($\delta 1$, $\delta 2$, $\delta 3$, $\delta 4$), but only three attitude degrees of freedom (ξ, η, ς), they are combined, mathematically to form the three control commands as follows [3]:

$$\xi = \frac{1}{4}(\delta_1 + \delta_2 + \delta_3 + \delta_4)$$

$$\eta = \frac{1}{4}(-\delta_1 - \delta_2 + \delta_3 + \delta_4) \qquad (1)$$

$$\varsigma = \frac{1}{4}(\delta_1 - \delta_2 - \delta_3 + \delta_4)$$

Figure 1. Positive deflection of control fins viewed from rear

Four positive fin deflections create a negative roll command; the first two fins up (negative) and the last two fins up (positive) generate a positive normal force command; and the fins 2&3 negative deflections with fins 1&4 positive deflections cause a positive yaw command. This convention can be summarized in the following:

Roll: $+\xi \rightarrow -\Delta L$ (negative rolling moment).

Pitch: $+\eta \rightarrow +\Delta N$ (positive normal force).

Yaw: $+\varsigma \rightarrow +\Delta Y$ (positive side force).

Here using six degree of freedom model to study all specification of the missile performance then must make linearization to be able to deal with the system as linear time invariant to design the controller and achieve time response parameter and frequency margins required. studying linearization of model to find the final transfer function of roll, pitch and yaw channels and then start to design controllers as required[6].

1. Linearization of missile model

Because the nonlinear state models are difficult to handle, most of the early progress in understanding the dynamics of missile and the stability of the motion came from studying linear small perturbation equations. When a computer simulation is performed to evaluate the performance of the missile with its control systems, a nonlinear model shall almost invariably be used. The linear equations needed for control system design will be derived using the small perturbation method from the nonlinear model. Considering the velocity derivatives as state variables and the acceleration as an output [2], the six equations can be written in state space form as follows:

$$
\begin{bmatrix} \Delta \dot{u} \\ \Delta \dot{v} \\ \Delta \dot{w} \\ \Delta \dot{p} \\ \Delta \dot{q} \\ \Delta \dot{r} \end{bmatrix} = \begin{bmatrix} X_u & 0 & 0 & 0 & 0 & 0 \\ 0 & Y_v & 0 & 0 & 0 & (Y_r - u_0) \\ 0 & 0 & Z_w & 0 & (u_0 + Z_q) & 0 \\ 0 & 0 & 0 & L_p & 0 & 0 \\ 0 & 0 & M_w & 0 & M_q & 0 \\ 0 & N_v & 0 & 0 & 0 & N_r \end{bmatrix} \begin{bmatrix} u \\ v \\ w \\ p \\ q \\ r \end{bmatrix} + \begin{bmatrix} 0 & 0 & 0 \\ 0 & 0 & Y_\zeta \\ 0 & Z_\eta & 0 \\ L_\xi & 0 & 0 \\ 0 & M_\eta & 0 \\ 0 & 0 & N_\zeta \end{bmatrix} \begin{bmatrix} \xi \\ \eta \\ \zeta \end{bmatrix} \quad (2)
$$

$$
\begin{bmatrix} \Delta a_x \\ \Delta a_y \\ \Delta a_z \\ p \\ q \\ r \end{bmatrix} = \begin{bmatrix} X_u & 0 & 0 & 0 & 0 & 0 \\ 0 & Y_v + l_p N_v & 0 & 0 & 0 & Y_r + l_p N_r \\ 0 & 0 & Z_w - l_p M_w & 0 & Z_q - l_p M_q & 0 \\ 0 & 0 & 0 & 1 & 0 & 0 \\ 0 & 0 & 0 & 0 & 1 & 0 \\ 0 & 0 & 0 & 0 & 0 & 1 \end{bmatrix} \begin{bmatrix} u \\ v \\ w \\ p \\ q \\ r \end{bmatrix} + \begin{bmatrix} 0 & 0 & 0 \\ 0 & 0 & Y_\zeta + l_p N_\zeta \\ 0 & Z_\eta - l_p M_\eta & 0 \\ 0 & 0 & 0 \\ 0 & 0 & 0 \\ 0 & 0 & 0 \end{bmatrix} \begin{bmatrix} \xi \\ \eta \\ \zeta \end{bmatrix} \quad (3)
$$

Then, the transfer functions will be:

$$
G_\zeta^{a_y} = \frac{a_y}{\zeta} = \frac{(Y_\zeta + l_p N_\zeta)s^2 + (N_v Y_\zeta l_p - N_\zeta Y_v l_p + N_\zeta Y_r - N_r Y_\zeta)s - N_\zeta Y_v u_0 + N_v Y_\zeta u_0}{s^2 - (N_r + Y_v)s + N_v u_0 - N_v Y_r + N_r Y_v} \quad (4)
$$

$$
G_\eta^{a_z} = \frac{a_z}{\eta} = \frac{(Z_\eta - l_p M_\eta)s^2 + (M_\eta Z_w l_p - M_w Z_\eta l_p + M_\eta Z_q - M_q Z_\eta)s + M_\eta Z_w u_0 - M_w Z_\eta u_0}{s^2 - (M_q + Z_w)s - M_w u_0 - M_w Z_q + M_q Z_w} \quad (5)
$$

$$G_\xi^p = \frac{p}{\xi} = \frac{L_\xi s - X_u L_\xi}{s^2 - (L_p + X_u)s + L_p X_u} = \frac{L_\xi(s - X_u)}{(s - L_p)(s - X_u)} = \frac{L_\xi}{(s - L_p)} \tag{6}$$

$$G_\eta^q = \frac{q}{\eta} = \frac{M_\eta s - M_\eta Z_w + M_w Z_\eta}{s^2 - (M_q + Z_w)s - M_w u_0 - M_w Z_q + M_q Z_w} \tag{7}$$

$$G_\varsigma^r = \frac{r}{\varsigma} = \frac{N_\varsigma s - N_\varsigma Y_v + N_v Y_\varsigma}{s^2 - (N_r + Y_v)s + N_v u_0 - N_v Y_r + N_r Y_v} \tag{8}$$

It is noticed that Equations (5 and 7) represent the two degrees of freedom short period approximation for the vehicle dynamics. Also, Equations (4 and 8) represent the two degrees of freedom Dutch roll approximation while equation (6) with the two equations (4 and 8) represent the three degrees of freedom Dutch roll approximation [1, 2, 3 and 4].

2. Choice of trim conditions

Before designing an autopilot, the points on the trajectory at which the designer needs to investigate the performance of the missile must be chosen. the trim points should be at different flight conditions during the rocket motor powered and unpowered stages to avoid repeating the design points [3]. In order to select the design points, the Mach number and altitude must be plotted with the flight time, or instead of them the dynamic pressure can be introduced with the change of flight time and trajectory as shown in Fig. 2.
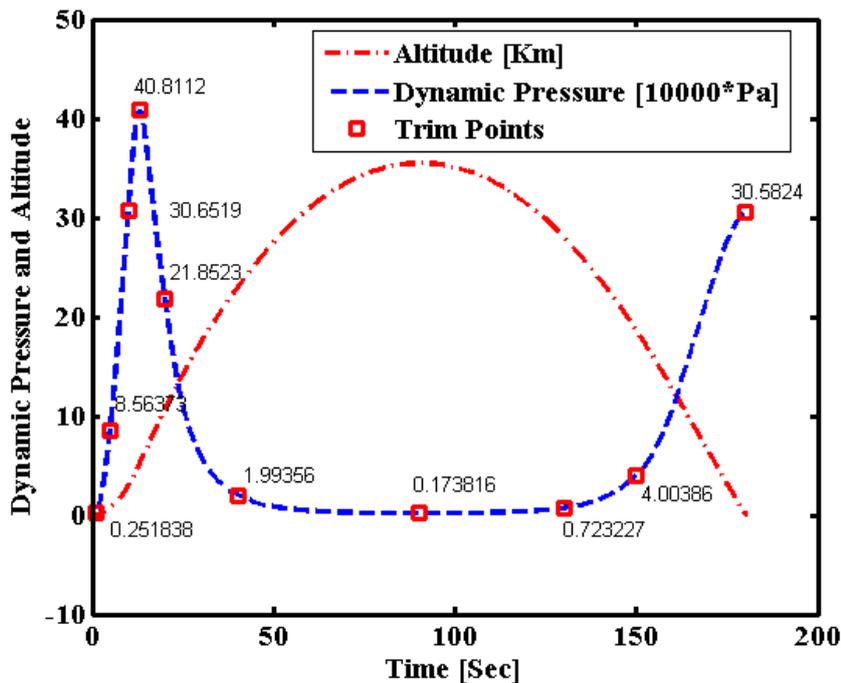

Figure 2. Change of dynamic pressure and altitude during flight

As shown in Fig.1:

- At the first seconds the change in altitude and dynamic pressure is almost small.
- The dynamic pressure reaches its maximum value at the end of powered phase at time (t=13.05 sec).
- The dynamic pressure decreases at the beginning of the unpowered phase.
- Before the altitude reaches summit and at time (t=60sec), Qbar remains almost with constant value till time (t=120 sec) during passing through the summit.
- After 120 sec the dynamic pressure returns to increase due to increasing of atmospheric density and velocity till reaching the target point.

This discussion clarifies that the designing points can be chosen as follows:

2.1. During the powered phase:

- Choice of (1 sec.) point at which the missile leaves the launcher and the boost phase of the rocket engine thrust has been finished with the small and disturbed change in parameters have been passed[7][8].
- Due to rapid change in dynamic pressure and missile states during the powered phase, a point will be selected at every 5 sec.
- Thus, the points are (1 sec), (5 sec), (10sec) and (13.05 sec).

2.2. During the unpowered phase:

- Due to moderate change in dynamic pressure and missile parameters, this phase will be divided into regions with mid and final-points for each region are selected[9].
- First region at which dynamic pressure decreases, a point at the beginning is chosen (13.05 sec) and the points of (20 sec) at the mid and (40 sec) at the end.
- Second region at which dynamic pressure changes slightly, one point is sufficiently at the mid (90 sec).
- Third region at which dynamic pressure increases, a point at the beginning is chosen (90 sec), the mid-point at (150 sec) and the end at (180 sec).

Then the set of designing points are shown in table 1.which clarify the design points located on the Mach number, altitude and dynamic pressure curves.

Table 1. Set of designing points

point	1	2	3	4	5	6	7	8	9
Time [sec]	1	5	10	13.05	20	40	90	150	180
Mach	0.188	1.1477	2.5	3.317	3.591	2.887	2.19	2.894	2.088
Altitude [m]	22	730	3021	5169	10598	22955	35461	18524	109
Q_{bar} [Pa]	2518	85640	306545	408153	218575	19952	1742	40208	305857

3. Calculation of Aerodynamic Transfer Functions

Introducing the trim conditions at each point, the coefficients of the aerodynamic transfer functions can be calculated [4]. The trim condition is that point at which the missile flies without pitching moment, i.e. (Cm=0). Due to symmetric shape of the airframe about $Cx_B y_B$ plane, the trim state occurs when the flow is symmetric about this plane, i.e. at zero angle of attack (α=0) and this condition is valid only for zero angles of fins deflection. The values of non-dimensional aerodynamic derivatives and aerodynamic transfer functions at trim points are as in equation 6, 7, 8. Stability and control derivatives are derived as functions of Mach number, where both the angle of attack and the sideslip angle are equal zero. The aerodynamic derivatives and then the corresponding aerodynamic transfer functions are calculated at design points. From Datacom software, it will be acceptable if choosing between points (2) or (3) or (5) or (8). The dynamic parameters at points (3), (5) and (8) are very high, and then it will be suitable if choosing point (2). Finally, point (2) is chosen at time (t=5sec) to be the nominal design point [3,10,11].

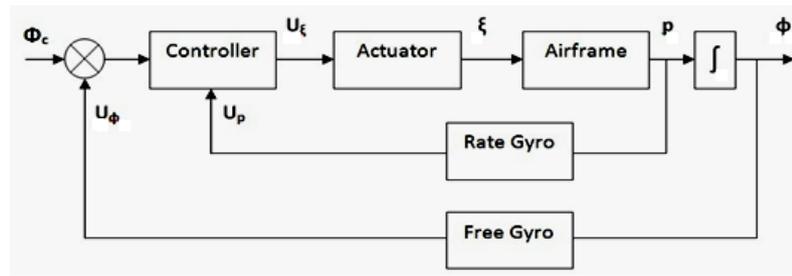### 4. Design of Roll Autopilot

The basic function of the roll autopilot is to roll-rate stabilize the missile, that is, to provide missile stabilization of roll attitude about the longitudinal axis. This is accomplished by sensing roll rate, and using the signal to deflect the fins by an amount sufficient to counteract roll disturbances. Moreover, the response of the system must be sufficiently fast to prevent the accumulation of significant roll angles. With skid-to-turn control, the missile is preferred to remain in the same roll orientation as at launch during the whole flight. If up-down guidance signals are sent to the elevator servos, these results in a vertical maneuver of the missile; and if left-right signals are sent to the rudder servos results in a horizontal maneuver. However, if there is no roll control, the missile has no tendency to remain in the same roll orientation[5][6]. In fact, it will tend to roll due to any of the following causes:

- Accidental assembling errors which cannot be eliminated entirely.
- Asymmetrical loading of the lifting and control surfaces in supersonic flight which occur when pitch and yaw angles of attack occur simultaneously and are not equal.
- Atmospheric disturbances especially if the missile is flying close to the ground.

A block diagram of the roll autopilot is shown in [5], which consists of two loops:

- The inner loop is designed to damp any undesired roll-rate utilizing a spring-restrained rate gyroscope for roll rate measurement, in conjunction with a specified compensator. This loop is designed in the form of stability augmentation system in order to increase the damping of the whole autopilot and damp any sudden roll.
- The outer loop is designed to track the roll angle of missile which is required to be zero utilizing a free vertical gyroscope as an attitude reference. This loop is designed in the form of control augmentation system in order to track the value of the commanded rolling angle[7][12].

The value of commanded rolling angle ϕ_c is sent from the guidance computer, and then the controller collects the signals fed back from rate gyro and that one from the free gyro (or navigation computer) to properly sum them with the commanded signal (φ_c). The controller processes these summed signals to produce the control signal (U_ξ) which actuates the hydro-electric actuator to obtain the corresponding aileron deflection angle (ξ). In the simulation, the distribution law will be derived to show how these four actuator signals will be combined [8][13].

Figure 3. Block diagram of roll autopilot[14]

4.1. Inner loop design

Inner loop consists of some block diagrams as a subsystem   each block represent apart and has a function in the loop to accumulate and achieve loop function as described before in the following, we will show every part in the loop and its transfer function.
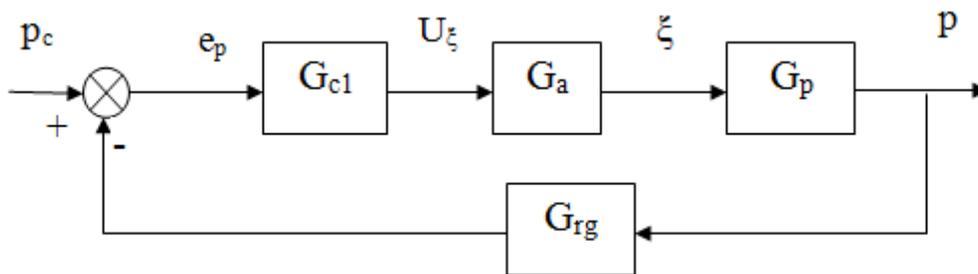
Figure 4. Roll autopilot inner-loop

From the airframe transfer function, we must calculate it at definite time that choosing before it is changed with time here, we calculate at t=5sec.

Considering the airframe transfer function at (t = 5 sec):

$$G_p = G_\xi^p = \frac{p}{\xi} = \frac{-319.7}{s + 0.4128} \tag{9}$$

In addition, considering first-order lag actuator and unity gain rate-gyro yields: The main function of the actuator is to achieve the control command that used to make the loop function commanded from servo and deflect to damp the roll effect and its transfer function is:

$$G_a = \frac{25}{s+25}, \qquad G_{rg} = 1 \tag{10}$$

Then, the open-loop transfer function G_{op} is obtained:

$$G_{op} = \frac{-7992.5}{s^2 + 25.4128s + 10.32} = \frac{-7992.5}{(s + 0.4128)(s + 25)} \tag{11}$$

Here we find open loop transfer function and then study the time and frequency responses to study all system response and find a method for design. It's better to introduce negative feedback at

the summation point and negative gain at the forward path to obtain positive DC gain and make the action of the output signal in the same direction of the input signal[4][15].
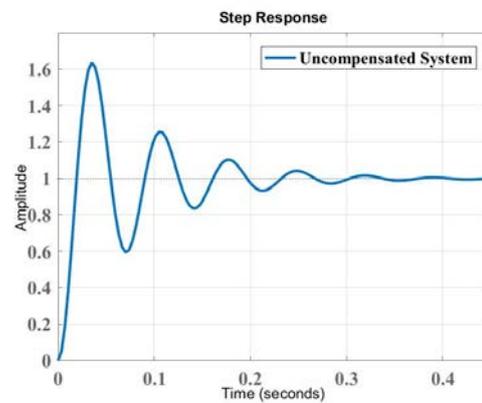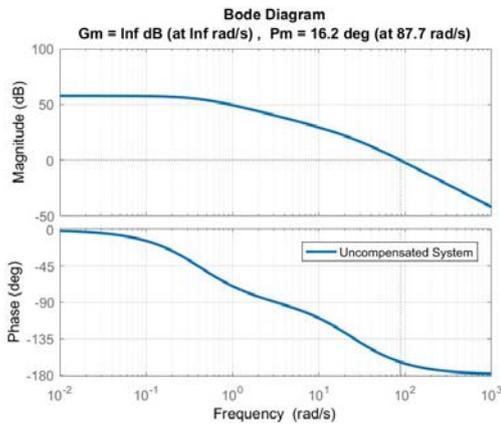
Figure 5. Bode plot of inner-loop transfer function   **Figure 6.** Step response of the uncompensated system

From the figures above finding that the open loop response has frequency response: Gain margin=inf dB, Phase margin=16.2 deg. which mean that the system is unstable.

Time response parameter is: Over shoot = 63.7%, rise time=0.0131 sec, settling time=0.292 sec.

Since we have specific requirement in the inner loop function to do its function:

The performance requirements needed for the inner-loop are:

- Damping ratio $0.4 \leq \zeta \leq 0.7$.
- M.O. < 10%.
- GM > 10 dB & PM > 45˚.
- Steady-state error $e_{ss} < 0.01$

The relative stability characteristics (PM > 45˚), can be achieved by adding phases to the system shown in Fig. 5 and this can be done phase-lead compensator. Since the phase margin equals (16.2˚) and the required phase margin is 45˚, then at least 28.8˚ must be added to the system at gain cross-over frequency to achieve the required stability margins. If the minimum phase has to be added is 30°, let $(\phi_m) = 30°$ and then (a) will be obtained by:

$$a = \frac{1+\sin(\phi_m)}{1-\sin(\phi_m)} = \frac{1+\sin(35)}{1-\sin(35)} = 3.7$$

The gain added in this case is:

$$G_\infty = 20\log_{10} a = 20\log_{10} 3.7 = 11.36 \ dB$$

The gain at (ω_m) equals half of G_∞, i.e. The gain cross over frequency is =123 rad/sec

$$G_m = \frac{G_\infty}{2} = \frac{11.36}{2} = 5.68 \ dB$$

Once (a) is determined, it is necessary only to determine the value of (T), and the design is in principle completed. This is accomplished by placing the corner frequencies of the phase-lead controller, (1/aT and l/T), such that (ϕ_m) is located at the new gain-crossover frequency (ω_g') so the phase margin of the compensated system is benefited by (ϕ_m).

Thus, in order to locate the new gain crossover at (ϕ_m) which is the geometric mean of (1/aT) and (1/T), it is needed to place (ω_m) at the frequency where the magnitude of the uncompensated $(1/a)*G_{op}(j\omega)$ is -5.68dB. So that, adding the controller gain of 5.68 dB to this makes the magnitude curve go through 0 dB at ω_m. From Fig. 5, the uncompensated gain $G_{op}(j\omega)$ equals -10dB, and the frequency ω_m equals 116 rad/s. Thus the parameter (T) is given by[9][16]:

$$T = \frac{1}{\omega_m \sqrt{a}} = \frac{1}{123\sqrt{3.7}} = 0.00423$$

Now, the transfer function of the phase-lead controller becomes:

$$G_{c1} = \frac{1+aTs}{1+Ts} = \frac{1+3.7*0.00423s}{1+0.00423s} = \frac{1+0.01564s}{1+0.00423s}$$

The forward-path transfer function of the compensated system is:

$$G = G_{c1}G_{op} = \frac{29551.5(s+64)}{s3+261.813s2+6017.92s+2439.65}$$

The frequency response shows that the phase margin of the compensated system is actually 46.7°. Checking the time-domain performance of the compensated system yields the following results:

- M.O. = 26.2%
- Rise time tr = 0.00953 sec.
- Settling time ts = 0.0433 sec.
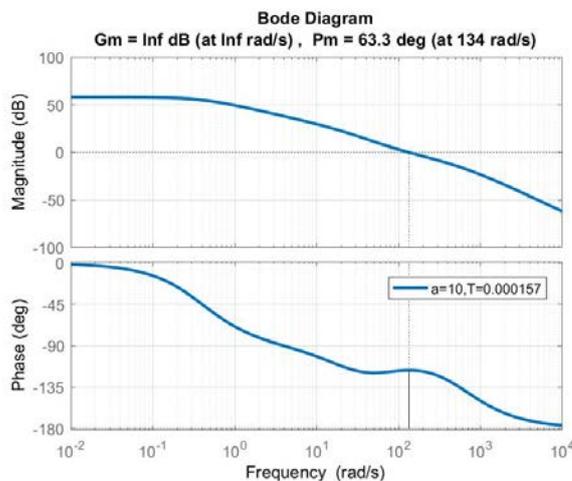


Figure 7. The frequency response for the inner loop
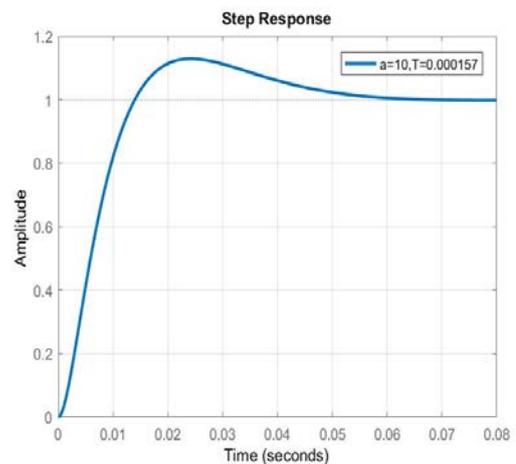
Figure 8. The time response

| a	T	Gain margin (GM)	Phase margin (PH)	Overshoot	Rise time	Settling time	Corner frequency
-	-	∞	16.2deg	63.7%	0.0131	0.292	87HZ
3.7	0.00423	∞	46.7deg	26.7%	0.00956	0.0519	123HZ
10	0.000157	∞	63.7deg	13.1%	0.00953	0.0433	157HZ

A comparative analysis has been conducted to evaluate the proposed design approach and ensure the most suitable compensator that ensure high performance while preserving the system stability

during the flight. The gain margin here in the inner loop is not a main parameter. Time response parameter is more important here[17].
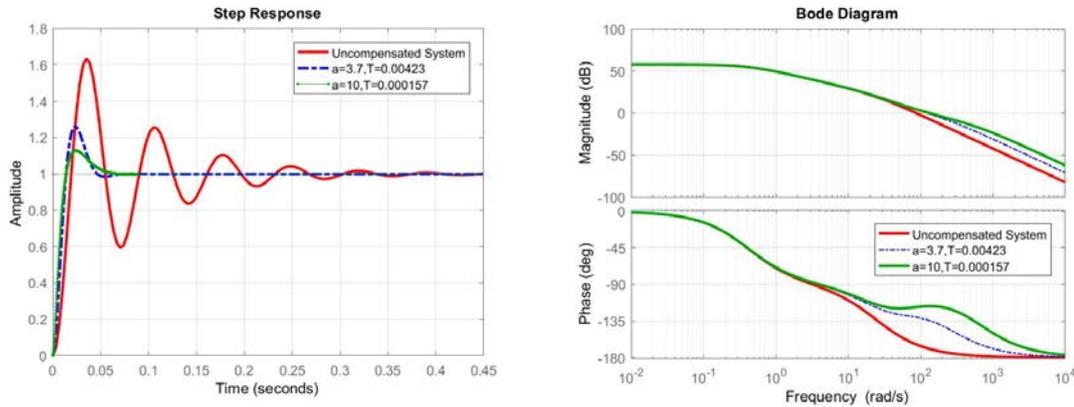
Figure 9. Time and frequency response comparison with and without compensator

This loop includes integrator factor which makes the whole system of type-1 and the steady-state error of the whole system equals to zero[10][6]. The block diagram of the outer loop is shown in fig.9.
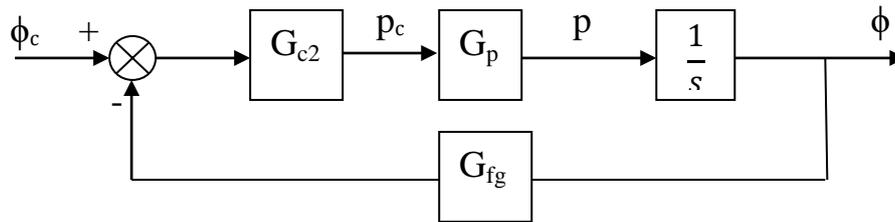
Figure 10. Block diagram of roll outer loop.

The value of free gyro gain G_{fg} equals unity and the transfer function of the feedback inner loop is:

$$G = G_{c1}G_{op} = \frac{79925(s+64)}{s^3 + 662.4s^2 + 16198.3s + 6573.84}$$

The forward-path transfer function G_{fp}:

$$G_{fp} = \frac{79925(s+64)}{s^4 + 662.4s^3 + 16198.3s^2 + 6573.84s}$$

The integrator in the loop is to make steady state error equal zero that's required to the outer loop to do its function .so we here instead of using PI controller we use P controller only to obtain our required response.

Here we show the effect of value of P controller and outer loop design for roll autopilot design for our missile. First, we take value of controller gain with equal one and then calculate response and control if we will increase value or no. Controller gain = K and K=1 (unity gain of controller).
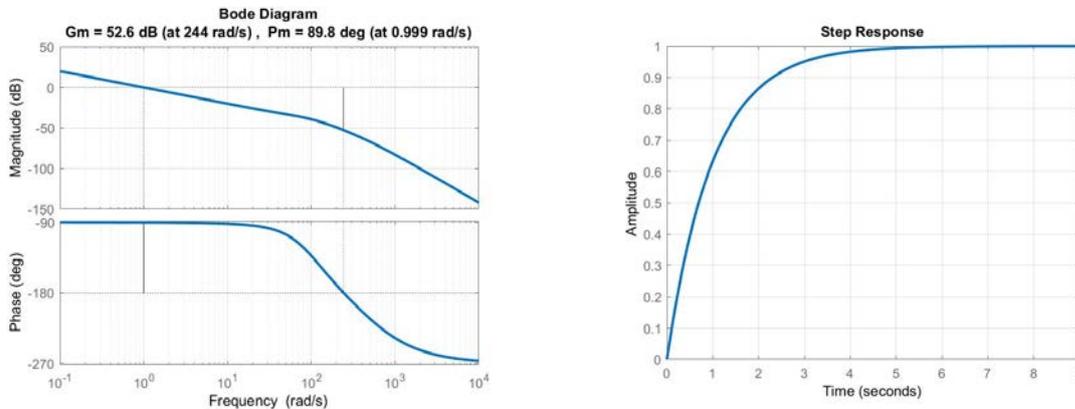
Figure 11. System time and frequency response of all system at gain K=1

The results obtained with K=1 clarifies that:

- Gain margin = 52.6 dB
- Gain crossover frequency = 1 [rad/s]
- M.O. = 0%
- t_s = 3.91 sec.

- Phase margin = 89.8°
- Phase crossover frequency = 237 [rad/s]
- t_r = 2.19sec

The gain margin and phase margin are very large and this makes the system to be over damped as shown in [7]. In order to reduce the gain and phase margin, the gain can be increased and this will decrease the damping ratio and decrease the value of rise time and settling time. The two imaginary poles have damping ratio 0.707 at gain K=42.8.

The ramp error e_v is expressed as:

$$e_v = \frac{1}{k_v}$$

Where k_v is the velocity error constant and equals to:

$$k_v = \lim_{s \to 0} sG_{fp} = \lim_{s \to 0} \frac{79925(\,s + 64)K}{s^3 + 662.4s^2 + 16198s + 6573.84} = \frac{5115200K}{6573840} = 0.778K$$

Then for ramp error e_v to be less than 0.02 i.e.:

$$\frac{1}{0.778K} < 0.02 \Rightarrow K > \frac{1}{0.01556} \Rightarrow K > 64$$

Hence, changing the gain starting from K = 65 till obtaining the required stability margins and time response characteristics. The values of parameters with change of K after some trails to change the gain value to obtain required response we at the final choose value of gain controller equal(k=90).

The results obtained with K=90 clarifies that:
- Gain margin = 13.6 dB
- Phase margin = 48.5°

- Gain crossover frequency = 244 [rad/s]
- M.O. = 17.6%
- t_s =0.0762 sec.

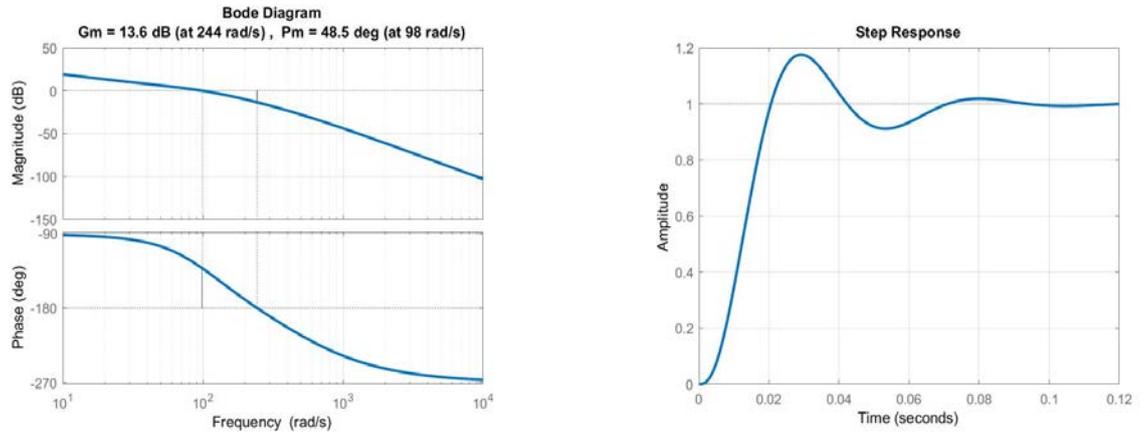- Phase crossover frequency =98[rad/s]
- t_r = 0.0129sec

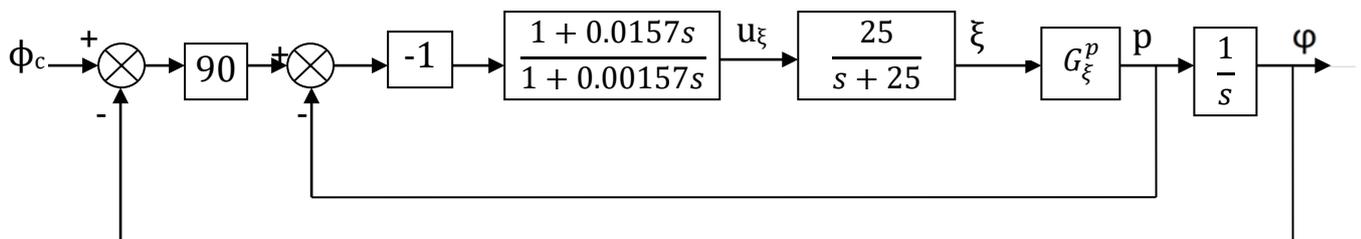**Figure 12**. System time and frequency response of all system at gain K=90

Figure 13. The block diagram of roll autopilot

5. Evaluation of designed roll autopilot

If a closed-loop system remains stable in the face of uncertainties, then the system is said to possess stability robustness. If the performance of a closed-loop system in the face of uncertainties is acceptable, then that system is said to possess performance robustness. Robustness, both stability and performance, can be tested for quite simply by investigating system response at each design point using the designed controller. The structure of the roll autopilot is the same for all design points except for the roll rate due aileron deflection transfer function G_ξ^p. The forward path transfer function G_{fp} of the autopilot is:

$$G_{fp} = \frac{-2250(1+.0157s)G_\xi^p}{s[(s+25)(1+.00157s) - 25(1+.0157s)G_\xi^p]}$$

We can also test our controller at any trim point and then check stability at this point to check that the controller is valid and effective and reliable at all points on flight curve.

6.Conclusion

In this paper, we proposed an efficient and simple procedure for designing roll autopilot control system starting from the 6DOF model for surface to surface missile which introduces high dynamics that makes the controller design is a challenging problem. The linearization of the model is fulfilled for designing a proper controller as well as this work presented a procedure for choosing the operating points around which the system behavior is almost linear based on the dynamic pressure as presented in section 3 and Fig. 2., 9 points have been chosen. The paper also introduced the design steps to obtain optimal controller at all trim points in the inner loop to make it stable utilizing lead compensator based on time response parameters (maximum overshoot, rise time and settling time) as well as frequency response parameters (gain and phase margins). Due to integrator in the outer loop we use proportional controller instead of proportional-integrator (PI)controller. A simulation is carried out for testing the designed controller under Matlab platform for testing the proposed controller design which presented good efficiency, robustness and performance for different design points and different flight conditions. The presented procedure presented advantages of simplicity of design beside the availability for implementation in real world applications with low processing complexity which made it an efficient approach for design roll autopilot. The work in this paper can be extended by integrating the designed controllers into a gain scheduling controller and also mapping the designed controller to digital form which made the design more reliable for implementation on embedded computers.

Reference

[1]   L. Sun, D. Li, and K. Y. Lee, "Optimal disturbance rejection for PI controller with constraints on relative delay margin," ISA Trans., vol. 63, pp. 103–111, 2016.

[2]   P. H. Zipfel, Modeling and Simulation of Aerospace Vehicle Dynamics, Second Edition. 2007.

[3]   B. L. Stevens and F. L. Lewis, Aircraft Control and Simulation, vol. 76, no. 5. 2004.

[4]   D. McRuer, I. Ashkenas, D. Graham, and I. McRuer, Duane;Graham, Dunstan;Ashkenas, Aircraft Dynamics and Automatic Control. 1973.

[5]   Ninth Edition Farid Golnaraghi • Benjamin C. Kuo. .

[6]   S. Srivastava and V. S. Pandit, "A PI/PID controller for time delay systems with desired closed loop time response and guaranteed gain and phase margins," J. Process Control, vol. 37, pp. 70–77, 2016.

[7]   K. Elkobbah, M. S. Mohamed, and A. M. Bayoumy, "Comparison of Classical and Predictive Autopilot Design for Tactical Missile Nomenclature :," 2013.

[8]   M. K. ELBAIOUMY, Mohamed Misbah Elkhatib, A. E. KHALIFA "Modelling and Simulation of Surface-to-Surface Missile General Platform", Advances in Military Technology, 2018, Vol.13, No.2, PP 277-290, DOI 10.3849/aimt.01236, ISSN 1802-2308, eISSN 2533-4123.

[9]   B. S. Kim and A. J. Calise, "Nonlinear Flight Control Using Neural Networks," J. Guid. Control. Dyn., vol. 20, no. 1, pp. 26–33, 1997.

[10]   Z. Y. Nie, Q. G. Wang, M. Wu, and Y. He, "Tuning of multi-loop PI controllers based on gain and phase margin specifications," J. Process Control, vol. 21, no. 9, pp. 1287–1295, 2011.

[11]   Shawky A, Zydek D, Elhalwagy Y Z and Ordys A 2013 Modeling and nonlinear control of a flexible-link manipulator Appl. Math. Model. 37 9591–602

[12]   Metiaf A, Elkazzaz F, Hong W Q and Abozied M 2018 Multi-objective Optimization of Supply Chain Problem Based NSGA-II- Cuckoo Search Algorithm Multi-objective Optimization of Supply Chain Problem Based NSGA-II-Cuckoo Search Algorithm

[13]   Hendy H, Rui X, Zhou Q and Khalil M 2014 Controller Parameters Tuning Based on Transfer Matrix Method for Multibody Systems 2014

[14]   Elkazzaz F S and Abozied M A H 2017 Hybrid RRT / DE Algorithm for High Performance UCAV

Path Planning 235–42

[15]   Hendy H, Rui X and Khalil M 2013 An Integrated GPS / INS Navigation System for land vehicle 338 221–6

[16]   Nonlinear U Q and Laws C 2016 Modeling And Simulation of Spacecraft Pointing Modes 1–14.

[17]   Abozied M, Abozied H and Qin S High performance path following for UAV based on advanced vector field guidance law 555–64.